Fotoprzewodnictwo i fotodetektory.

"Podstawy fizyczne elektroniki ciała stałego", Aldert van der Ziel
"Physics of Semiconductor Devices" S.M.Sze

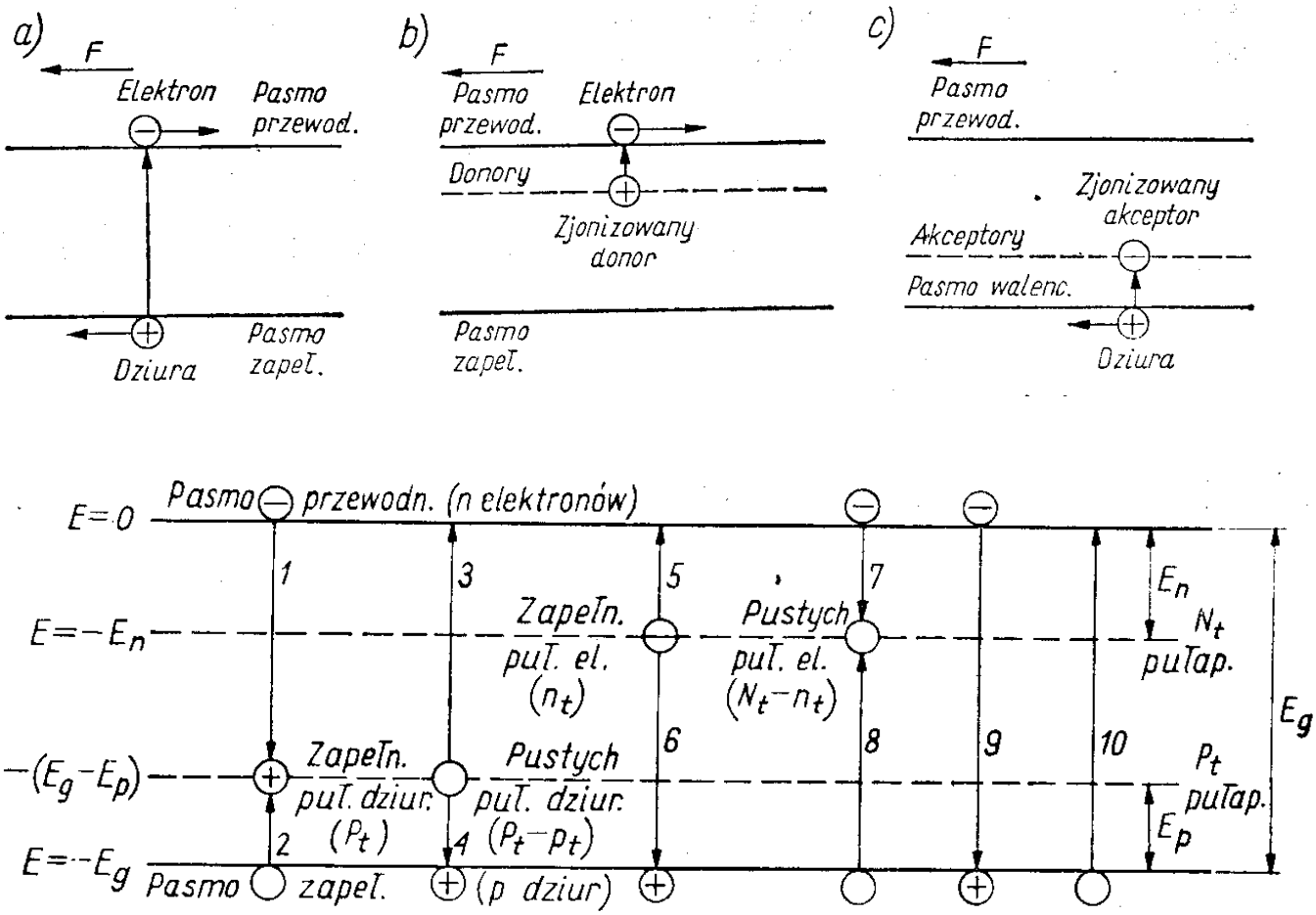

Rys. 11.5. Wykres poziomów energetycznych dla półprzewodnika, w którym znajdują się pułapki elektronowe i dziurowe; różne możliwe przejścia są oznaczone cyframi 1, ..., 10; na rysunku podano także gęstości elektronów, dziur oraz pułapek

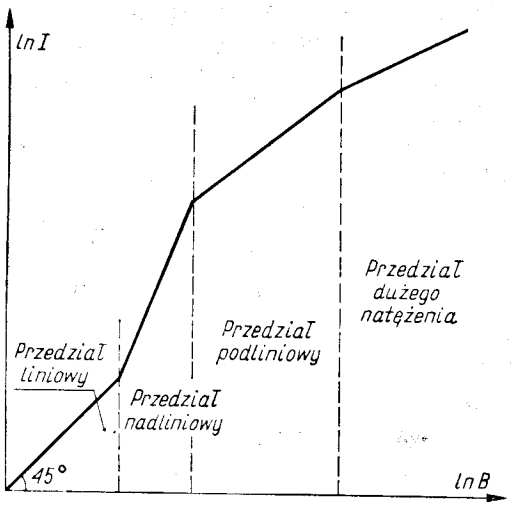

Rys. 11.6. Zależność fotoprądu I od natężenia światła B; zaznaczono przedziały: liniowy, nadliniowy, podliniowy oraz dużego natężenia

Table 1 Typical Values of Gain and Response Time

Photodetector	Gain	Response Time (s)	Operating Temperature (K)
Photoconductor	$1 \sim 10^6$	$10^{-3} \sim 10^{-8}$	$4.2 \sim 300$
p-n junction	1	10^{-11}	300
p-i-n junction	1	$10^{-8} \sim 10^{-10}$	300
Metal–semiconductor diode	1	10^{-11}	300
Avalanche photodiode	$10^2 \sim 10^4$	10^{-10}	300
Bipolar phototransistor	10^2	10^{-8}	300
Field-effect phototransistor	10^2	10^{-7}	300

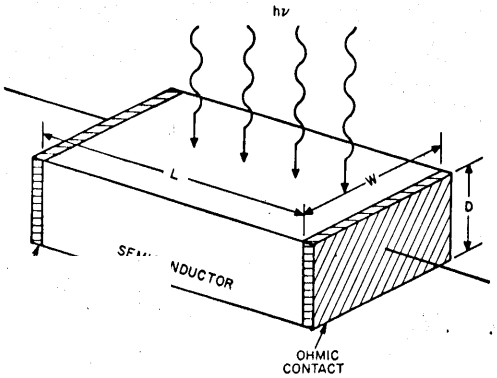

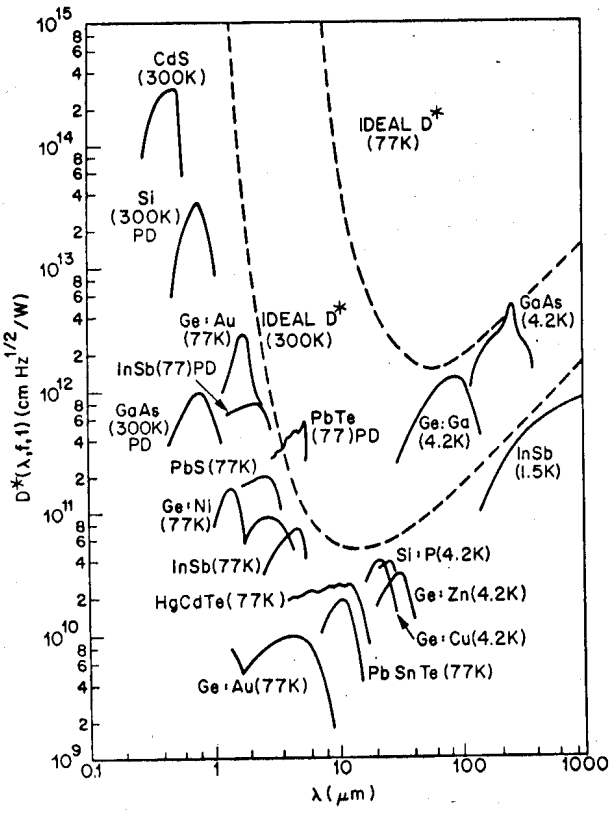

Fig. 4 Detectivity D^* as a function of wavelength for various photoconductors and photodiodes (indicated with PD). The dashed curves are the theoretical ideal D^* at 77 K and 300 K viewing an angle of 2π steradians. (After Kruse, McGlauchlin, and McQuistan, Ref. 12; Melchior, Refs. 2 and 3.)

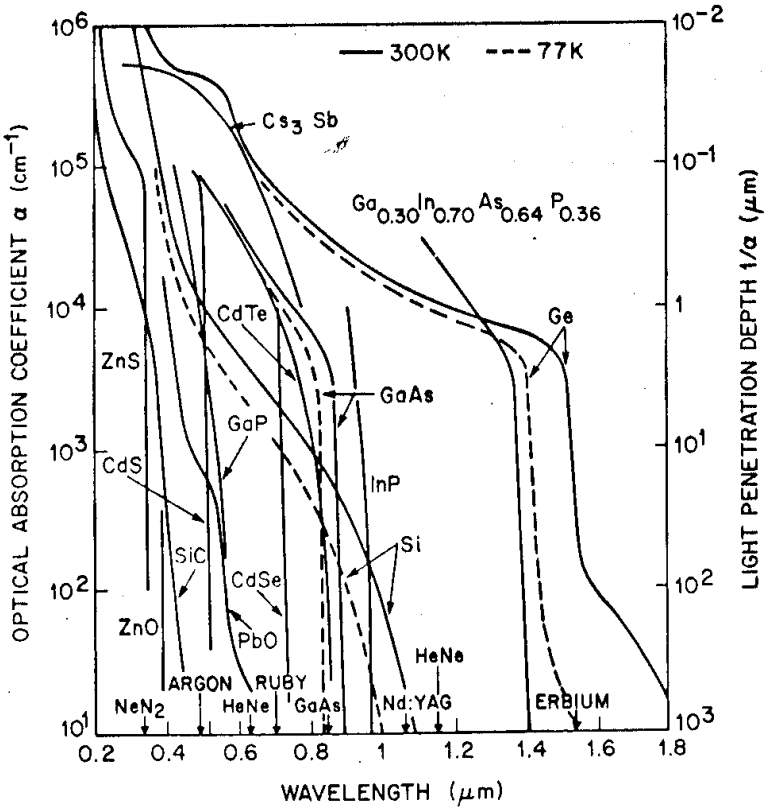

Fig. 5 Optical absorption coefficients for various photodetector materials; some laser emission wavelengths are indicated. (After Melchior, Ref. 2.)

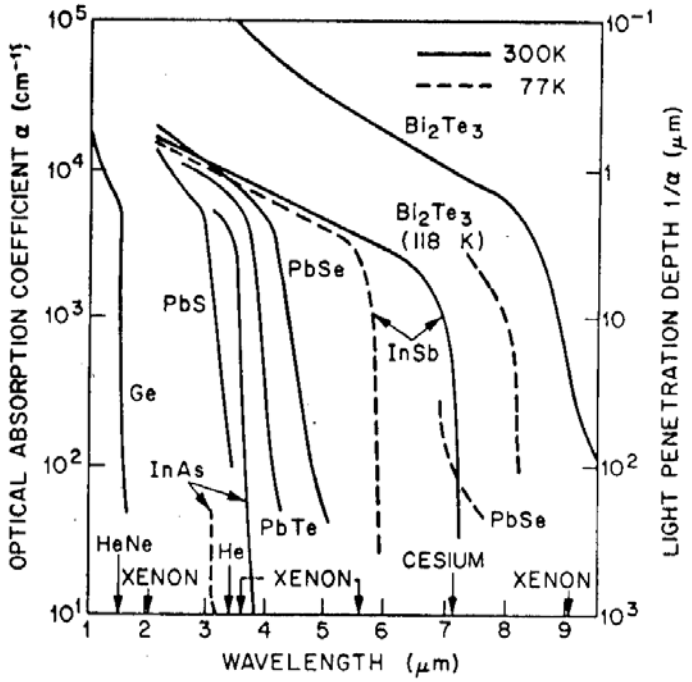

Fig. 6 Optical absorption coefficients for infrared photodetector materials. (After Melchior, Ref. 2.)

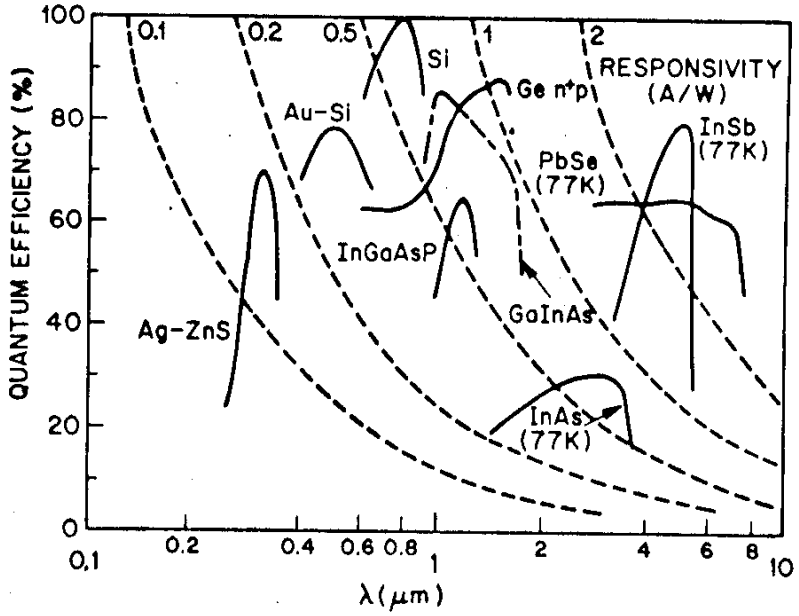

Fig. 7 Quantum efficiency and responsivity for various photodetectors.

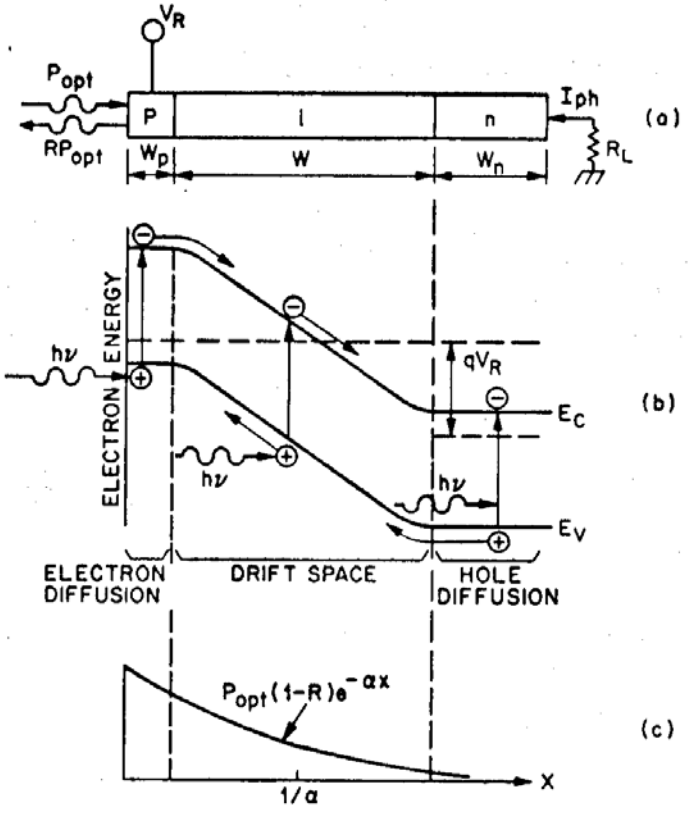

Fig. 10 Operation of photodiode. (a) Cross-sectional view of *p-i-n* diode. (*b*) Energy-band diagram under reverse bias. (*c*) Carrier generation characteristics. (After Melchior, Ref. 2.)

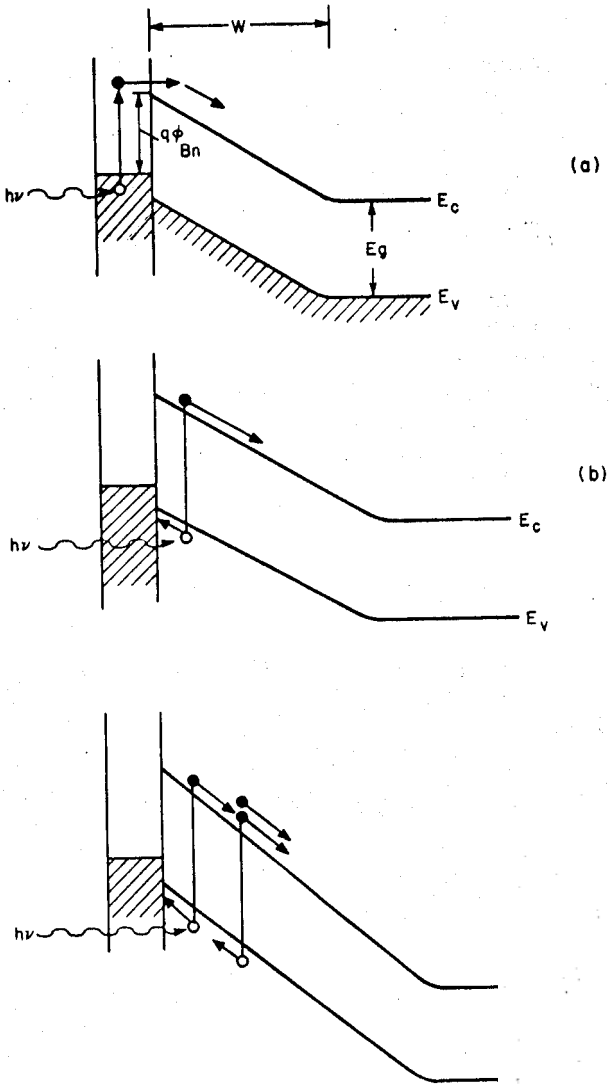

Fig. 14 (a) Photoelectric emission of excited electrons from ($E_g > h\nu > q\phi_{Bn}$). (*b*) Band-to-band excitation of a hole–ele Hole–electron pair generation and avalanche multiplication u ($h\nu > E_g$ and $V \simeq V_B$).

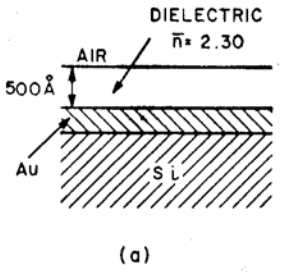

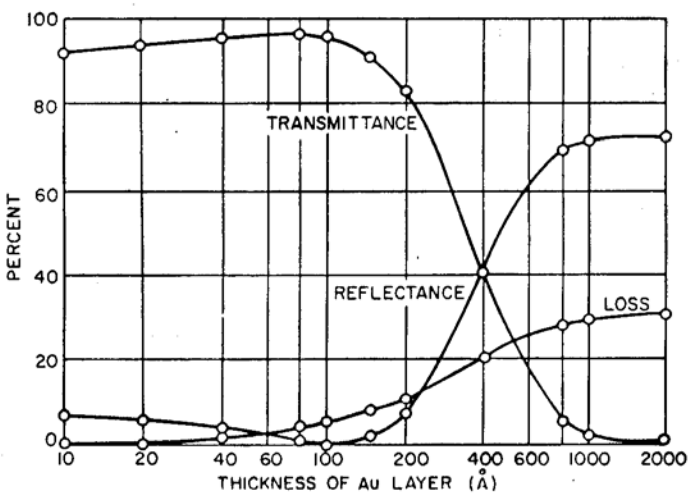

Fig. 15 (a) A 500-Å-thick ZnS antireflection coating. (*b*) Transmittance, reflectance, and loss in the gold films as a function of the gold layer thickness, $\lambda = 0.6328\ \mu m$. (After Schneider, Ref. 19.)

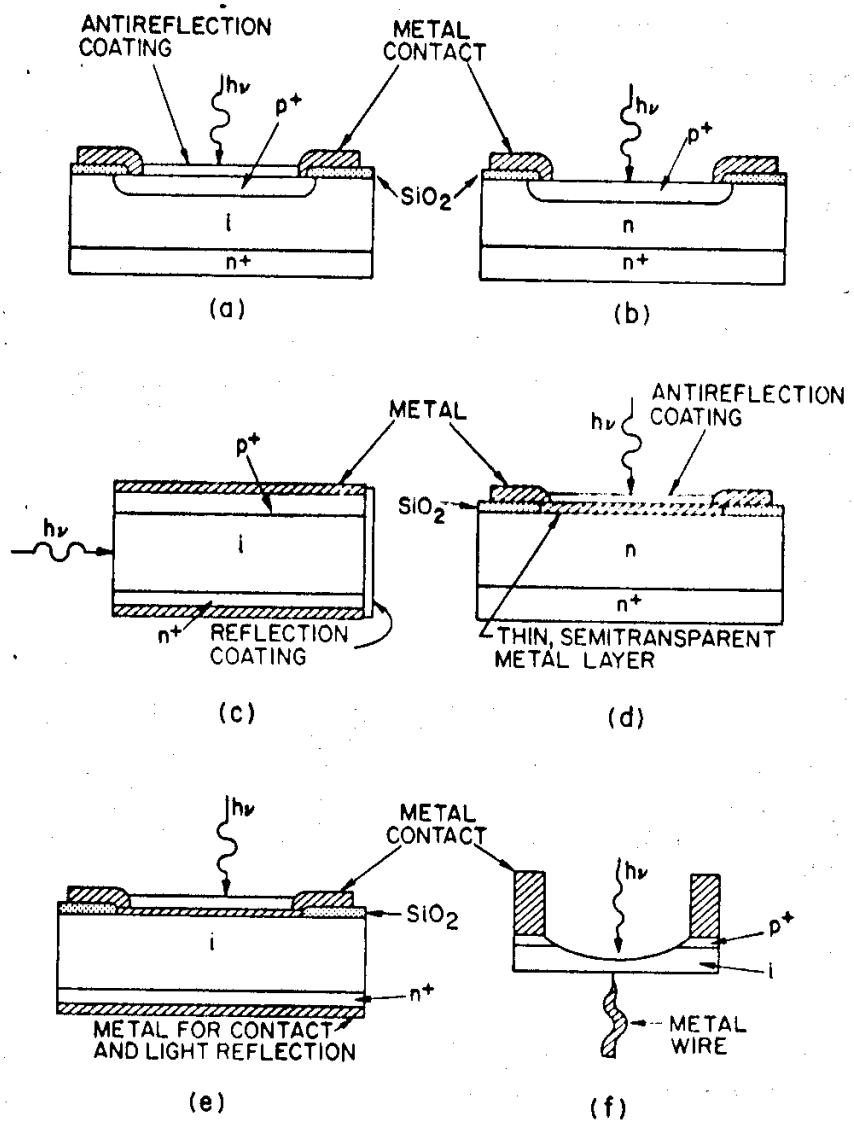

Fig. 13 Device configurations of some high-speed photodiodes. (*a*) *p-i-n* diode. (*b*) *p-n* diode. (*c*) *p-i-n* diode with illumination parallel to junction. (*d*) Metal–semiconductor diode. (*e*) Metal–*i*-*n* diode. (*f*) Semiconductor point-contact diode. (After Melchior, Ref. 2.)

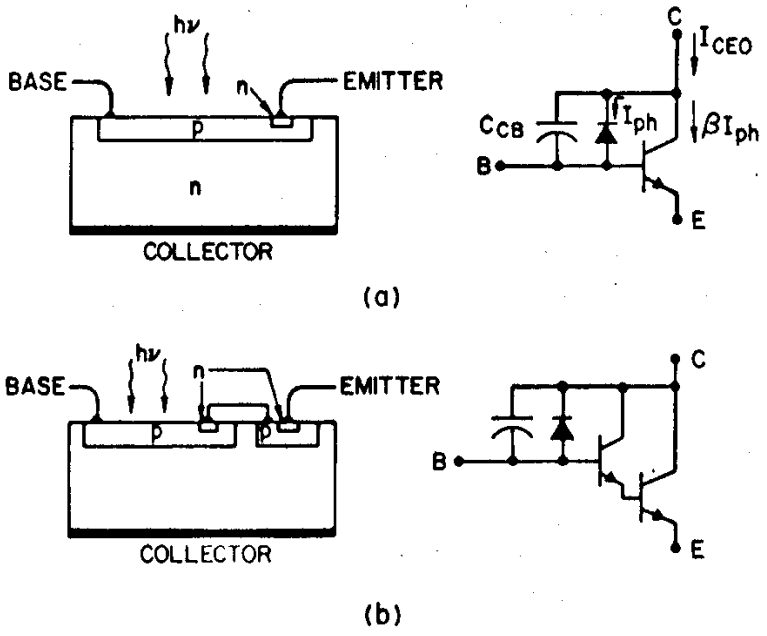

Fig. 33 (*a*) Bipolar phototransistor. (*b*) Photo-Darlington. (After Jayson and Knight, Ref. 51.)

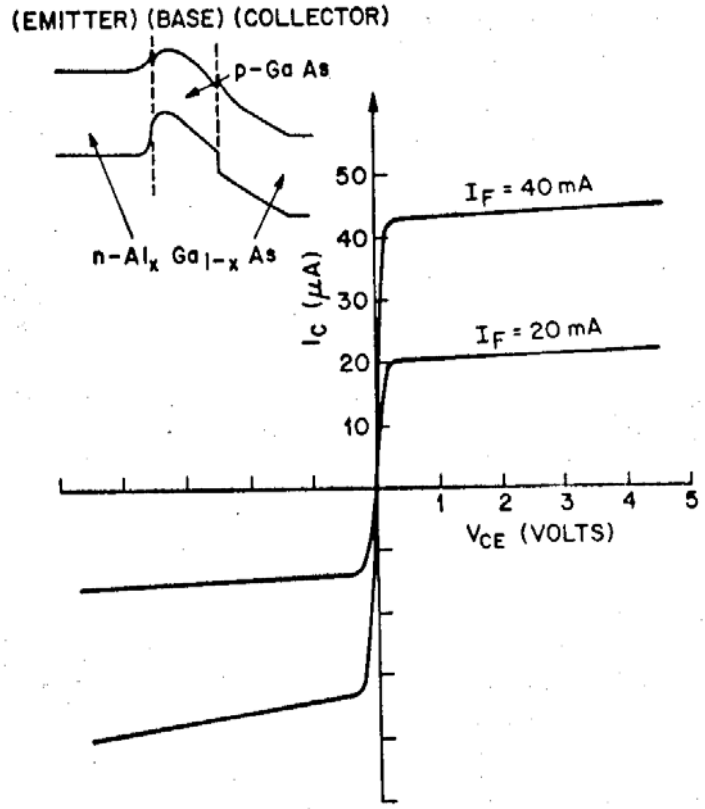

Fig. 34 Current-voltage characteristics of a bilateral heterostructure phototransistor. (After Knight et al., Ref. 53.)